nature communications

Article

https://doi.org/10.1038/s41467-026-71740-1

Adipocytes signal to recruit specific mRNAs from surrounding cells to restore expression deficits

Received: 8 April 2024

Accepted: 31 March 2026

Published online: 11 April 2026

Check for updates

Clair Crewe[1,2,3] ✉, Christy M. Gliniak[3,4], Toshiharu Onodera[3,5], Shiuhwei Chen[3], Jan-Bernd Funcke[3], May-Yun Wang[3], Snigdha Tiash[1,2], Yun-Ling Pai[1,2], Marjori Russo[1,2], Saket Awadhesbhai Patel[1,2], Ze Yu[6], Yi-Cian Zheng[1,7], Alex Larkin[1], Chao Xing[6,8,9], Laurent Gautron[10], Chun-Kan Chen[1], Chen Liu[10] & Philipp E. Scherer[3]

Extracellular vesicles (EVs) are nano-sized, membrane-delimited, particles released by cells that carry signaling macromolecules. A major pathway of EV production is potentiated by neutral sphingomyelinase 2 (SMPD3/nSMAse2), an enzyme that generates ceramide from sphingomyelin. In our attempt to study this pathway in adipocytes of male mice, we discover that the elimination of SMPD3 from adipocytes in vivo triggers a signal to surrounding immune cell-like preadipocytes to release EVs that carry SMPD3 mRNA. This results in a widespread increase in SMPD3 mRNA in purified null adipocytes without a change in the transcripts of other enzymes involved in ceramide metabolism. These results point to a selective mechanism by which specific mRNA molecules are acquired from the microenvironment to a level that can restore expression of mRNA and protein in a cell that is depleted of the corresponding genetic information.

Extracellular vesicles are released from cells and carry all classes of macromolecules, including proteins, RNAs, DNA, and metabolites, enclosed in a lipid bilayer[1]. This diversity of cargo results in dramatic changes in the function of receiving cells as EVs can signal at all levels simultaneously: transcription, translation, and signal transduction[1]. EVs are now known to play a significant role in the progression of multiple diseases including cardiovascular disease, obesity and type 2 diabetes, neurodegeneration, and cancer[2–5]. Adipocyte-derived EVs have a disease-promoting signaling effect in the obese setting. Hypertrophic, insulin-resistant adipocytes produce EVs that induce insulin resistance in myocytes and adipocytes and activate macrophages to a proinflammatory phenotype[6]. We have shown that EVs from dysfunctional adipose tissue propagate disease phenotypes to the liver and have an overall negative effect on systemic metabolism[7]. However, we have also demonstrated that adipocyte EVs released in the context of obesity that carry mitochondria can protect the heart from ischemia reperfusion injury[8].

Exosomes are a sub-class of EVs that are generated in the multivesicular body (MVB) when the limiting membrane buds to form intraluminal vesicles loaded with cellular cargo[1]. Fusion of the MVB

[1]Department of Cell Biology and Physiology, Washington University School of Medicine, St. Louis, MO, USA. [2]Department of Internal Medicine, Division of Endocrinology, Metabolism and Lipid Research, Washington University School of Medicine, St. Louis, MO, USA. [3]Touchstone Diabetes Center, University of Texas Southwestern Medical Center, Dallas, TX, USA. [4]Department of Nutritional Sciences, Rutgers, The State University of New Jersey, New Brunswick, NJ, USA. [5]Department of Adipose Management, The University of Osaka, Graduate School of Medicine, Osaka, Japan. [6]McDermott Center of Human Growth and Development, The University of Texas Southwestern Medical Center, Dallas, TX, USA. [7]Cancer and Cell Biology Program, Baylor College of Medicine, Houston, TX, USA. [8]Department of Bioinformatics, The University of Texas Southwestern Medical Center, Dallas, TX, USA. [9]O'Donnell School of Public Health, The University of Texas Southwestern Medical Center, Dallas, TX, USA. [10]Center for Hypothalamic Research, University of Texas Southwestern Medical Center, Dallas, TX, USA. ✉e-mail: clair.crewe@wustl.edu

https://doi.org/10.1038/s41467-026-71740-1

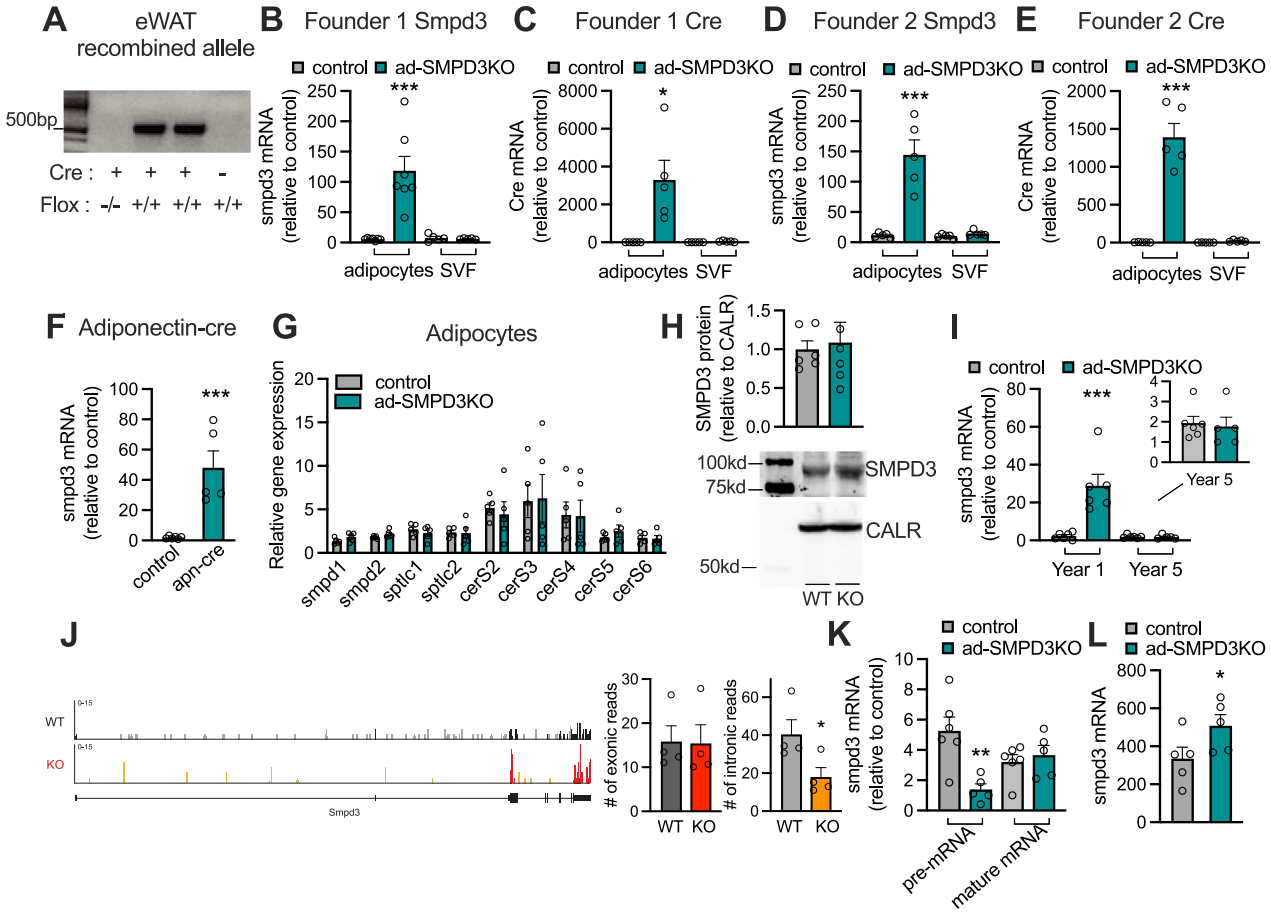

Fig. 1 | Adipocyte-specific SMPD3 knockout. A PCR product of eWAT DNA with primers for the recombined Smpd3^{flox} allele (representative of $n = 7$). ad-SMPD3KO mice were placed on a chow diet containing 600 mg/kg doxycycline for 2 weeks. sWAT tissue was dissociated from ad-SMPD3KO mice derived from two independent Smpd3^{flox} founder lines to separate mature adipocytes from the stromal vascular fraction (SVF). qPCR was conducted on these fractions for Smpd3 mRNA (**B** adipocyte control $n = 7$ vs. adipocyte ad-SMPD3KO $n = 7$, $P = 0.0005$; SVF control $n = 5$ a SVF ad-SMPD3KO $n = 5$ and **D** $n = 5$, adipocyte ad-SMPD3KO, $P = 0.0007$) and Cre mRNA (**C** adipocyte control $n = 5$ vs. adipocyte ad-SMPD3KO $n = 5$, $P = 0.0131$ and (**E** adipocyte control $n = 5$ vs. adipocyte ad-SMPD3KO $n = 5$, $P < 0.0001$). **F** Smpd3^{flox} mice were crossed to mice carrying the constitutive adiponectin-Cre transgene, adipocytes were isolated from sWAT, and Smpd3 mRNA was quantified (control $n = 6$; ad-SMPD3KO $n = 5$, $P = 0.0014$). **G** qPCR on adipocytes from the sWAT of ad-SMPD3KO mice for genes encoding proteins involved in ceramide metabolism ($n = 5$). **H** Western blot analysis of SMPD3 protein in isolated adipocytes from control (WT; $n = 6$) or ad-SMPD3KO (KO; $n = 6$) mice. **I** Smpd3 mRNA expression in adipocytes at 1 year vs 5 years after receiving founders (year 1 control $n = 6$, year 1 ad-SMPD3KO $n = 6$, $P = 0.0015$; year 5 control $n = 6$; year 5 ad-SMPD3KO $n = 5$). **J** Sequencing data for the Smpd3 mRNA from control (WT) or ad-SMPD3KO (KO) sWAT adipocytes ($n = 4$, 3 separate experiments, $P = 0.049$). **K, L** 4 days after doxycycline-induced SMPD3 knockout, qPCR was performed on isolated sWAT adipocytes (**K**; Smpd3 mature mRNA or pre-mRNA; control $n = 6$; ad-SMPD3KO $n = 5$, $P = 0.0055$) or SVF (**L**; Smpd3 mature mRNA, $n = 5$, $P = 0.037$). Data are presented as mean ± s.e.m. Statistics by two-tailed Student's t test.

with the plasma membrane releases the intraluminal vesicles into the extracellular space, where they are then called exosomes. Exosomes are produced by two pathways: the endosomal sorting complex required for transport (ESCRT)-dependent pathway and the ESCRT-independent pathway. The latter relies on sphingomyelin phosphodiesterase 3 (SMPD3), also called neutral sphingomyelinase 2 (nSMase2), which catalyzes the conversion of sphingomyelin to ceramide, a lipid class required for generating the nano-sized membrane curvature of the intraluminal vesicles[9].

To study adipocyte exosome signaling we generate an adipocyte-specific SMPD3 loss-of-function mouse model. This leads to the surprising finding that knocking out SMPD3 in adipocytes stimulates an adipocyte-derived signal that recruits Smpd3 mRNA from surrounding cells, restoring expression. This may have important implications not only for preclinical gene manipulation in adipocytes, but also for disease states in which altered gene expression could be shaped by this recruitment process, either promoting physiological adaptation to stress or contributing to disease resistance or initiation.

Results

To study adipocyte EV signaling in obesity in vivo, we attempted to suppress adipocyte exosome release by knocking out SMPD3. We developed a conditional Smpd3 allele (Smpd3^{flox}) by inserting two loxP sequences flanking the endogenous exon 3. The floxed exon can be deleted in the presence of Cre recombinase. The Smpd3^{flox} mouse was crossed with mice carrying the adiponectin-rtTA and TRE-cre transgenes to generate an adipocyte-specific and doxycycline (DOX)-inducible model of Smpd3 ablation (ad-SMPD3KO mouse). We confirmed the genomic deletion of Smpd3 exon 3 in the epididymal white adipose tissue (eWAT) by PCR amplification of the recombined allele in mice that carried floxed SMPD3 alleles and expressed Cre in adipocytes (Fig. 1A). The subcutaneous white adipose tissue (sWAT) was then dissociated with collagenase to isolate mature adipocytes and the stromal vascular fraction (SVF). Isolated RNA from adipocytes was digested with DNAse and qPCR was conducted with primers for Smpd3 mRNA (exon 3) to verify SMPD3 knockout. To our surprise, Smpd3 mRNA was increased by over 100-fold in isolated ad-SMPD3KO

adipocytes with a disrupted SMPD3 gene compared to control cells (Fig. 1B, D). This effect was seen with 2 independent Smpd3^{flox} founder lines (Fig. 1B–E). We instead crossed the Smpd3^{flox} line with mice carrying an adiponectin-Cre transgene to generate an adipocyte-specific constitutive model of Smpd3 ablation. We observed the same substantial increase in Smpd3 mRNA in adipocytes isolated from these mice despite apparently full ablation of the gene (Fig. 1F). We also quantified the mRNA of other SMPD isoforms and other enzymes involved in ceramide metabolism in adipocytes from the ad-SMPD3KO mice. No changes were detected in either founder (Fig. 1G and data not shown), suggesting the strong up-regulation of Smpd3 in our knockout model is specific to this transcript. No change in SMPD3 protein was detected between genotypes in isolated adipocytes (Fig. 1H). Over years of breeding, the dramatic increase in Smpd3 mRNA we observed initially, was attenuated so that there was no change between WT and ad-SMPD3KO adipocytes by year 5 after founders were received (Fig. 1I). Even though the massive mRNA compensation was attenuated over time, at no stage could we identify "knock out" adipocytes that had lower than wildtype mRNA levels for SMPD3. Sequencing of the Smpd3 mRNA from purified adipocytes demonstrated that knockout adipocytes still have full length, mature mRNA with all exons represented equally (Fig. 1J). In contrast, pre-mRNA, represented by intronic reads, was lower in knockout mice (Fig. 1J), suggesting reduced de novo transcription of the SMPD3 gene within the ad-SMPD3KO adipocytes. We also demonstrated this by qPCR 4 days after the adipocyte knockout was induced. The pre-mRNA was significantly reduced in adipocytes but no change in mature mRNA was detected (Fig. 1K). Interestingly, there was a potentially compensatory increase in mature Smpd3 mRNA in the SVF fraction at this 4-day timepoint (Fig. 1L).

To validate that the Smpd3^{flox} line is indeed functional, we crossed it with mice carrying Rosa26-rtTA and TRE-Cre transgenes to generate a whole-body, DOX-inducible deletion model as well as with mice carrying an albumin-Cre transgene to generate a hepatocyte-specific constitutive deletion model. Smpd3 mRNA was depleted in the liver and sWAT in the whole-body model (Fig. 2A) and selectively in the liver for the hepatocyte-specific model (Fig. 2B). These data suggest that the floxed allele works as intended to produce SMPD3 knockout cells in the presence of Cre recombinase. However, in the adipocyte-specific model, the SMPD3 mRNA remains abundant. We have previously published a similar phenomenon where we attempted to eliminate caveolin-1 (CAV1) specifically in adipocytes[10]. In this model, the adipocyte was depleted of Cav1 mRNA but the protein was only reduced by 40–50%. We reported that EVs loaded with CAV1 protein from surrounding endothelial cells were taken up by adipocytes, replenishing adipocyte CAV1 levels. Therefore, we investigated whether Smpd3 mRNA is being transferred to adipocytes via EVs in our ad-SMPD3KO mice. As EV-associated mRNA uptake into adipocytes would likely result in cytoplasmic delivery, we reasoned that nuclear Smpd3 mRNA should be reduced in Smpd3 knockout adipocytes, consistent with the observed reduction in Smpd3 pre-mRNA (Fig. 1K). We homogenized purified adipocytes from the sWAT of control and ad-SMPD3KO mice, isolated a nuclei-enriched fraction, and measured SMPD3 mRNA with intron-spanning primers. Nuclear, mature Smpd3 mRNA was significantly reduced in the knockout mice (Fig. 2C). We next isolated small EVs (sEVs) from the sWAT (ATsEVs) to quantify Smpd3 mRNA cargo levels. These sEVs were isolated and characterized as previously described[10]. They ranged in size from 50–300 nm (Fig. 2D) and the total number of ATsEVs did not differ between genotypes (Fig. 2E). These ATsEVs displayed a heterogeneous morphology (Fig. 2F), typical of an EV population, and the isolate was devoid of any obvious cellular debris when imaged by electron microscopy (Fig. 2F and S1[10]). Smpd3 mRNA was detectable in ATsEVs and significantly increased in tissue sEVs from the ad-SMPD3KO mice compared to control mice (Fig. 2G). This data represents a snapshot of Smpd3 mRNA levels in ATsEVs at the time of isolation and does not account for the turnover (i.e., the rate of EV production from donor cells and the rate of EV uptake by recipient cells). Because Smpd3 is more highly expressed in SVF compared to adipocytes (Fig. 2H), the SVF cells are likely the source of ATsEV Smpd3 mRNA and may have the capacity to fully restore Smpd3 mRNA levels in adipocytes. To understand the range of mRNAs that are present in ATsEVs and whether the potential transfer of Smpd3 mRNA was accompanied by other mRNAs in the same cellular pathway, we performed an RNA sequencing analysis on ATsEVs from control and ad-SMPD3KO sWAT. 280 transcripts were increased, and 461 were decreased in ATsEVs from ad-SMPD3KO mice compared to those from control mice (Fig. 2I). Gene Ontology analysis revealed a striking enrichment of immune cell-related transcripts in the ad-SMPD3KO ATsEVs (Fig. 2J). The transcripts are related to both innate and adaptive immune cell activities. This data suggests enrichment of immune cell-derived EVs in the ATsEV pool, as EVs are generally thought to carry cell type-specific RNAs that reflect the physiological state of the producing cell[11]. No pathways that are canonically associated with SMPD3 expression or sphingolipid metabolism were identified.

The upregulation of Smpd3 mRNA in ad-SMPD3KO adipose tissue and the presence of Smpd3 mRNA in ATsEVs suggested that another cell type in the tissue may selectively package this mRNA into EVs for delivery to adipocytes. To test this, we first cultured the SVF cells from the sWAT of wildtype (WT) control and ad-SMPD3KO mice. Although the SVF is a composite of immune cells, fibroblasts, stem cells, and endothelial cells, the cells that propagate under the chosen culture conditions are enriched in adipocyte precursor cells. These cells can be differentiated into mature adipocytes. Given a differentiation efficiency of ~80%, we can use this relatively pure adipocyte culture to assess SMPD3 elimination. Following differentiation, we induced the SMPD3 knockout by the addition of 1 μg/ml DOX to the culture medium for 48 h and measured Smpd3 mRNA. The cells were trypsinized, and mature adipocytes were separated from other undifferentiated SVF cells. Unexpectedly, we did not detect any change in adipocyte Smpd3 mRNA, but we did see a modest increase in Smpd3 mRNA in the undifferentiated SVF (Fig. 3A). This suggested that the cell type responsible for replenishing adipocyte Smpd3 mRNA levels remains as part of the 10–20% of cells that do not differentiate into adipocytes in culture. If we extend the culture time from 2 days to 4 days, we can detect an accumulation of Smpd3 mRNA in both mature adipocytes and stromal cells (Fig. 3A). Furthermore, when we treated freshly isolated SVF with the conditioned media collected from ad-SMPD3KO adipocytes, Smpd3 mRNA was induced in the SVF compared to treatment with control adipocyte conditioned media (Fig. 3B). This upregulation of Smpd3 was not detected if the ad-SMPD3KO conditioned media was depleted of EVs and other dense particles by a 100, 000xg spin (Fig. 3B). These data suggest that there is a high density extracellular signal emanating from adipocytes that elicits the upregulation of Smpd3 mRNA in stromal cells and, potentially, promotes the transfer of Smpd3 mRNA back to adipocytes.

To directly test if Smpd3 mRNA is transferred from stromal cells to adipocytes in culture, we designed a molecular beacon (MB) that selectively base-pairs with Smpd3 mRNA. When the MB is not bound to its target mRNA, its stem-loop structure brings the 5′ fluorophore (Alexa Fluor 647) in proximity to the 3′ quencher (BHQ-2). When the MB binds its target, the fluorophore is separated from the quencher. Thus, fluorescence is detected only in the presence of the target mRNA (Fig. 3C). MB fluorescence was robustly detected in WT control SVF, but the signal was absent in SVF isolated from whole-body SMPD3KO mice, validating the specificity of the MB (Fig. 3D, E). SVF was transfected with the MB and seeded into the top compartment of a Transwell plate. Following recovery overnight, these cells were co-cultured with WT control or ad-SMPD3KO adipocytes in the bottom compartment (Fig. 3F). The Transwells had a pore size of 0.4 μm to preclude cell migration through the filter but allow soluble molecules and particles

https://doi.org/10.1038/s41467-026-71740-1

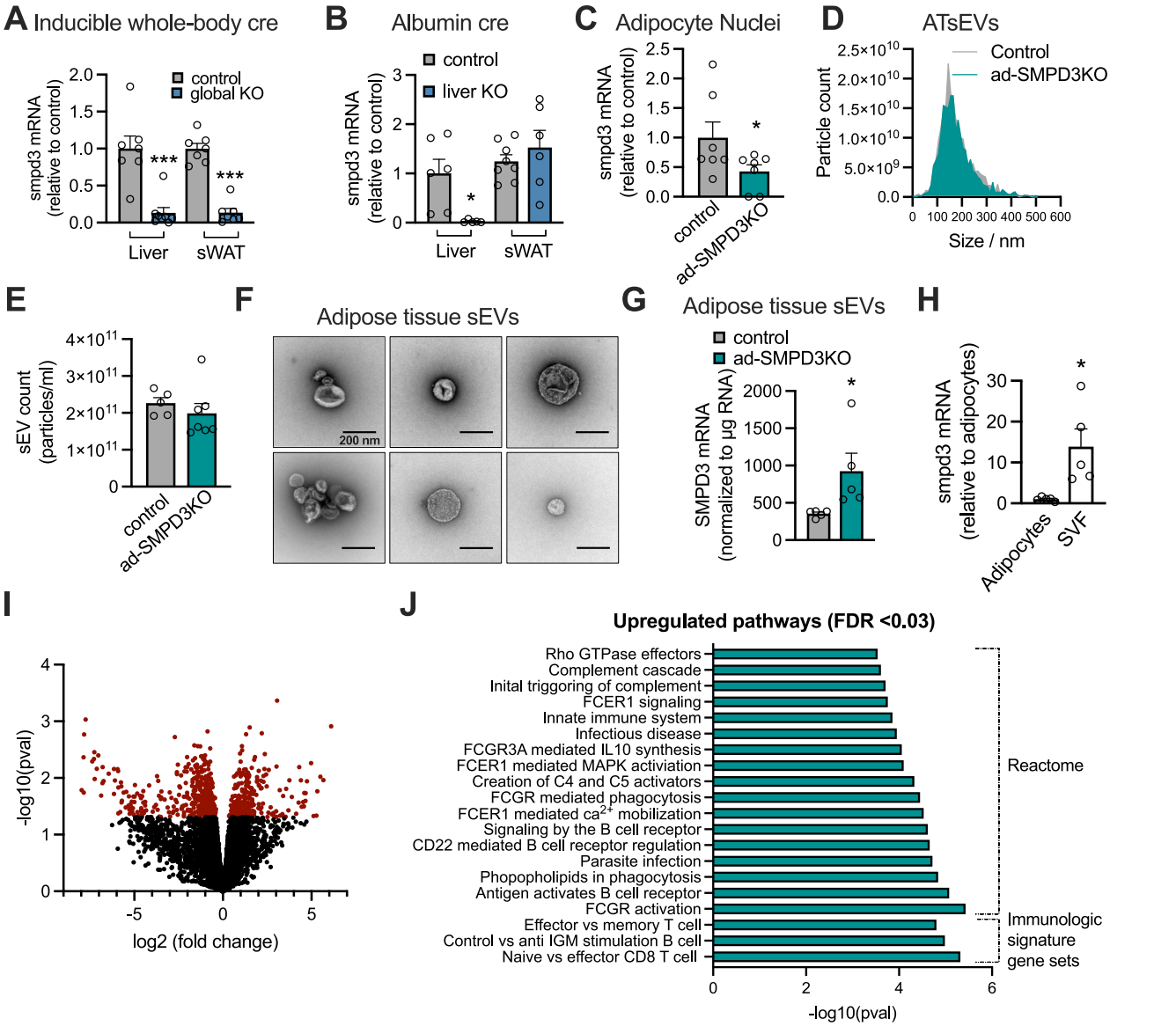

Fig. 2 | ad-SMPD3KO ATsEVs contain Smpd3 mRNA. The Smpd3^{flox} line was crossed to mice carrying Rosa26-rtTA and TRE-Cre transgene to obtain a doxycycline-inducible whole-body knockout (**A**; liver control $n = 7$ vs. liver knockout $n = 8$, $P = 0.0003$; sWAT control $n = 7$ vs. sWAT knockout $n = 7$, $P < 0.0001$) or to mice carrying an albumin-Cre transgene to obtain a constitutive hepatocyte-specific knockout (**B**; liver control $n = 6$ vs. liver knockout $n = 5$, $P = 0.014$; sWAT control $n = 8$; sWAT knockout $n = 6$). Smpd3 mRNA was quantified in the whole tissue. **C** adipocytes were isolated from the sWAT of control and ad-Smpd3KO mice, nuclei were purified, and qPCR was conducted for Smpd3 mRNA ($n = 7$), $P = 0.0361$. Adipose tissue small extracellular vesicles (ATsEVs) were isolated from the sWAT of control and ad-SMPD3KO mice and EV number and size distribution were quantified by nanoparticle tracking analysis (**D, E**; control $n = 5$; ad-SMPD3KO $n = 7$). **F** ATsEV morphology was assessed by electron microscopy, and **G** Smpd3 mRNA was quantified by qPCR ($n = 5$, $P = 0.046$). **H** Smpd3 mRNA expression in sWAT adipocytes vs. SVF ($n = 5$, $P = 0.018$). ATsEVs were analyzed by RNAseq. **I** Volcano plot illustrating differentially expressed genes between genotypes (red genes are significantly changed). **J** Gene ontology analysis of RNAseq data. Data are presented as mean ± s.e.m. Statistics by a two-tailed Student's t-test.

up to 400 nm to freely diffuse between compartments. After 24 h of co-culture, the MB was detectable in a small number of WT adipocytes compared to adipocytes co-cultured with mock-transfected SVF (Fig. 3G). Interestingly, transfer of the MB to ad-SMPD3KO adipocytes was significantly enhanced compared to the transfer to control adipocytes (Fig. 3G–I). Most cells that took up the MB were mature adipocytes (Fig. 3H). This mRNA transfer was not stimulated by a knockdown of SMPD3 by siRNA, suggesting the signal is derived from a change at the genetic level (Supplementary Fig. 2A-B). Finally, the increase in Smpd3 mRNA transfer to knockout adipocytes was not due to more EV release by SVF, or enhanced uptake by knockout cells. We microporated SVF cells with a CMV-nanoluciferase (Nluc)-HSP70 construct, which results in Nluc-HSP70 fusion protein incorporation into EVs as previously described[12]. Transfected SVF was co-cultured with control or ad-SMPD3KO adipocytes, and the luciferase activity was quantified in the media and adipocyte lysate after 24 h. No differences were seen between conditions (Supplementary Fig. 2C). This data suggests that knocking out SMPD3 in adipocytes induces a signal that instructs stromal cells to release Smpd3 mRNA without increasing overall EV release.

To demonstrate the transfer of Smpd3 mRNA in vivo, we transplanted a sWAT fat pad from whole-body SMPD3KO mice into a control recipient mouse (Fig. 3J). The knockout tissue was secured to the recipient's SWAT with sutures, and the fat pads were allowed to fuse

https://doi.org/10.1038/s41467-026-71740-1

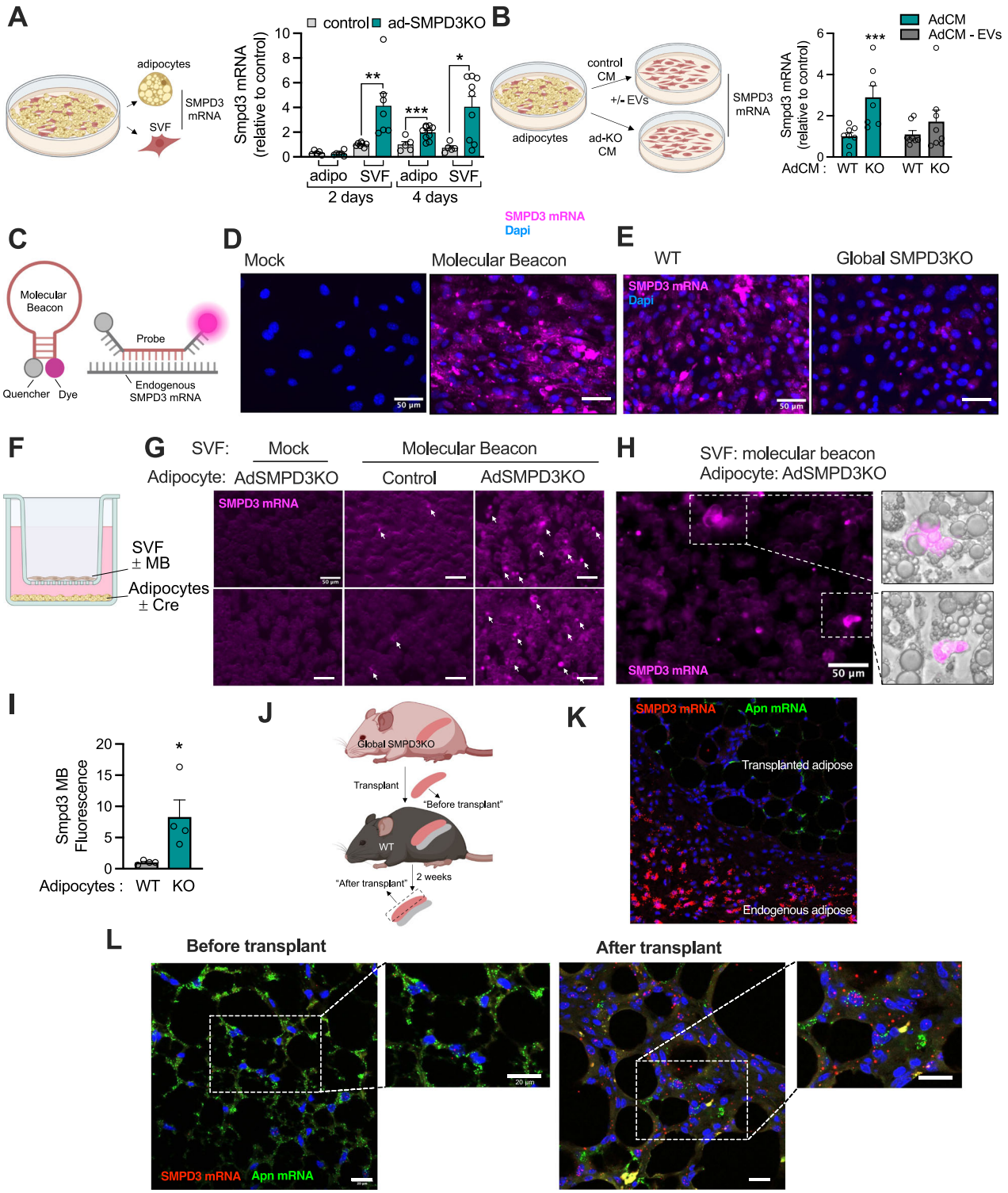

for 2 weeks. Following this recovery period, the fused fat pad was removed, processed for RNAscope, and stained with Smpd3 and adiponectin mRNA probes. The interface of the donor and recipient fat pads was clear, as the endogenous control tissue strongly stained for Smpd3 mRNA, whereas the transplanted knockout tissue was depleted of Smpd3 mRNA (Fig. 3K). Comparing SMPD3KO tissue before and after transplant, there was a clearly stronger signal for Smpd3 mRNA post-transplantation, localized to adiponectin-expressing adipocytes (Fig. 3L). This suggests that the donor SMPD3 knockout sWAT acquired Smpd3 mRNA from the recipient control tissue.

We subsequently performed a single-cell RNA sequencing experiment (scRNAseq) on all cells in the sWAT of control and ad-SMPD3KO mice to identify cells that highly expressed Smpd3 mRNA and therefore, may be candidate donor cells for Smpd3 mRNA transfer to adipocytes (Fig. 4A). The cell type that most highly expressed Smpd3 mRNA was a subpopulation of adipocyte progenitor cells (APCs) that has been previously described as PDGFRα^{+} and DPP4^{+} (Fig. 4B)[13]. This preadipocyte population is highly proliferative and multi-potent, which contrasts with the more committed adipocyte progenitors, which are PDGFRα^{+}, DPP4^{-}, and ICAM-1^{+}[13]. We FAC-sorted these two preadipocyte populations (CD45^{-}, PDGFRα^{+}, DPP4^{+} or Dpp4^{-};

Fig. 3 | Smpd3 mRNA is transferred from stromal cells to adipocytes. A Stromal vascular fraction (SVF) cells from sWAT were differentiated into mature adipocytes. SMPD3 was knocked out by addition of 1 μg/ml doxycycline to the medium for 2 or 4 days. Adipocytes were then separated from non-differentiated cells and Smpd3 mRNA expression was assessed by qPCR (2 days: adipo control $n = 5$; adipo KO $n = 6$; SVF control $n = 7$ vs. SVF KO $n = 7$, $P = 0.0094$. 4 days: adipo control $n = 5$ vs. adipo KO $n = 10$, $P = 0.005$; SVF control $n = 5$ vs. SVF KO $n = 9$, $P = 0.0141$). **B** Schematic illustrating the conditioned media (CM) experiment where media from control and ad-SMPD3KO adipocytes was used to treat SVF cells +/- EVs indicates whole CM (+ EVs) or CM cleared at 100, 000xg (-EVs). Following 24 h of treatment, Smpd3 mRNA was quantified in the SVF by qPCR (WT $n = 8$ vs. KO $n = 7$, $P = 0.0045$; WT-EV $n = 8$; KO-EV $n = 8$). **C** Illustration of the molecular beacon (MB) probe. **D** SVF cells from sWAT of control mice were electroporated with the MB or mock transfected. Following overnight recovery, cellular fluorescence was assessed (scale bar 50 μm; representative of N = 4, 3 separate experiments). **E** SVF from sWAT of control and whole-body SMPD3KO mice was electroporated with the MB and imaged 24 h later (scale bar 50 μm; representative of N = 4, 3 separate experiments). **F** Schematic illustrating the transwell co-culture experiment. SVF cells from sWAT of control and ad-SMPD3KO mice were differentiated into mature adipocytes and treated with 1 μg/ml doxycycline for 24 h prior to co-culture with MB or mock-transfected control SVF. **G** MB fluorescence detected in control (wild-type; WT) or ad-SMPD3KO adipocytes co-cultured with either MB or mock-transfected SVF (scale bar 50 μm). **H** Magnified image of the MB signal in ad-SMPD3 adipocytes (scale bar 50 μm). **I** Quantification of the MB signal in adipocytes ($n = 4$, $P = 0.037$, 3 independent experiments). **J** Schematic illustrating the adipose tissue transplantation experiment. **K** RNAscope image of sWAT at the interface of host and transplanted tissue (scale bar 20 μm). **L** RNAscope image of the sWAT from whole-body SMPD3KO mice before and after transplantation (representative of $n = 5$). The Smpd3 mRNA probe is shown in red and the adiponectin (Apn; adipocyte marker) probe in green. **K** and **L** are representative of 5 mice. Data are presented as mean ± s.e.m. Statistics by a two-tailed Student's t-test. Illustrations were Created in BioRender. Crewe, C. (2026) https://BioRender.com/ilz4odx, https://BioRender.com/66v3pgx, https://BioRender.com/twvrfgd, https://BioRender.com/qmpleme, https://BioRender.com/dehl8w0.

Supplementary Fig. 3) and repeated the MB transfer experiment using these cells instead of total SVF cells in the upper compartment. Unexpectedly, despite high Smpd3 mRNA expression in DPP4$^+$ APCs, we did not detect any transfer of the MB to ad-SMPD3KO adipocytes (Fig. 4C). We analyzed the scRNAseq dataset further and found that CD45 is highly induced in all APC populations in ad-SMPD3KO AT but not in immune cell populations (Fig. 4D). APCs expressing CD45 were excluded from the culture in Fig. 4C based on our FACS gating strategy (Supplementary Fig. 3). Smpd3 mRNA was not significantly changed in APCs from ad-SMPD3KO tissue although it trended to an increase (Fig. 4D). Gene ontology analysis suggests that APCs in the ad-SMPD3KO tissue display an immune cell-like, pro-inflammatory phenotype (Supplementary Fig. 4). Additionally, we found that both B cells and T cells express low levels of Smpd3 mRNA compared to APCs. However, there were more Smpd3 positive cells in these populations in ad-SMPD3KO tissue compared to control tissue. Both B and T cells have an activated phenotype in ad-SMPD3KO AT (Supplementary Fig. 4). The involvement of either bona fide immune cells or immune-modulating APCs in the transfer of Smpd3 mRNA to adipocytes is consistent with the ATsEV RNAseq data (Fig. 2J). Therefore, we bead-sorted CD45$^+$ cells (total immune cell population) from the SVF of sWAT and performed the transwell assay for MB transfer from the CD45$^+$ cells to WT or ad-SMPD3KO adipocytes. We found that CD45$^+$ cells displayed the same regulated transfer of Smpd3 mRNA as unsorted SVF (Fig. 3G), where little mRNA was transferred to control adipocytes, but Smpd3 mRNA accumulated robustly in knockout adipocytes (Fig. 4E). Although some Smpd3 mRNA was trafficked from CD45$^-$ cells to adipocytes, the extent was unaffected by the genotype of the recipient adipocyte (Fig. 4E). The cultured CD45$^+$ cells are almost all positive for Pdgfrα, suggesting that only APCs survived in culture. To test if APCs were the donating cell type in vivo, we crossed the ad-SMPD3KO mouse with the Pdgfrα-Cre mouse to knockout SMPD3 simultaneously in the mature adipocyte and pre-adipocytes ("doubleKO"). We found that the double knockout resulted in a significant reduction in Smpd3 mRNA in floated adipocytes compared to the up-regulation that occurs in the ad-SMPD3KO alone (Fig. 4G). These data suggest that CD45-positive APCs are the dominant donor cells for Smpd3 mRNA transfer to adipocytes.

These CD45$^+$ pre-adipocytes upregulate Smpd3 mRNA in response to ad-SMPD3KO adipocyte conditioned media compared to control adipocyte conditioned media (Fig. 5A, B), which is what we observed with SVF (Fig. 3B). This upregulation was mostly transcriptional as actinomycin D treatment prevented most of the increase in mature Smpd3 mRNA and completely suppressed the increase in pre-mRNA (Fig. 5A, B). Furthermore, Smpd3 mRNA accumulates in CD45$^+$ pre-adipocytes EVs. Using nanoparticle flow cytometry, we were able to detect the Smpd3 MB in CD45$^+$ cell extracellular particles. The number of MB-positive particles increased when CD45$^+$ cells were treated overnight with ad-SMPD3KO adipocyte-conditioned media compared to that from control adipocytes (Fig. 5C). Most of the MB signal was found in particles ~1 μm in size, suggesting the Smpd3 mRNA is in, or associated with EVs or large ribonuclear protein complexes (Fig. 5D). To determine if the mRNA is protected by a membrane, we repeated the MB transwell experiment with CD45$^+$ cells in the presence of RNase1 in the shared media. Interestingly, RNAse1 treatment did not affect the transfer of the MB to WT cells but reduced the MB transfer to knockout cells by ~50% (Fig. 5E). This suggests that there may be a basal level of Smpd3 mRNA transfer that is resistant to RNase. In response to the knockout, more Smpd3 mRNA is transferred by an RNase-sensitive mechanism. This could be either mRNA bound to the outside of an EV or large ribonuclear protein complexes.

Discussion

Our observations demonstrate that adipocytes can communicate a deficiency in Smpd3 mRNA to preadipocytes in their microenvironment, which respond by transferring more Smpd3 mRNA to adipocytes. This results in selective replenishment of the adipocyte Smpd3 mRNA pool. The mechanism by which this happens requires further investigation. mRNA transfer between cells has been reported to occur as protein-bound extracellular RNA, EV-enclosed RNA, or through tunneling nanotubules between adjacent cells and has been studied predominantly in the context of the tumor microenvironment[11,14]. The mRNA that is transferred can be translated or have translation-independent functions in the receiving cells[15,16]. The current understanding in the field is that small size, high abundance, cytoplasmic localization, and association with membranes and specific RNA-binding proteins favor the packaging of distinct RNAs into EVs[11]. Other factors are thought to influence the incorporation of RNAs into EVs, such as specific 3'UTR sequences, secondary structure, and modifications of the RNA or RNA-binding proteins[11]. Therefore, all RNA biotypes in EVs tend to reflect both the highly expressed, cell-type-specific RNAs in the producing cell and the physiological or pathological state of the cell. However, little is known about the regulation of mRNA tethering to the outer surface of the EV membrane. The extent to which RNA loading into or onto EVs is selective for specific RNAs, and whether this process is regulated, is unknown[11]. Based on this convention in the field, we would expect Smpd3 mRNA in pre-adipocyte EVs to be accompanied by transcripts encoding other proteins involved in sphingolipid metabolism. However, this is not the case. Instead, our data points to a mechanism that has the potential to be highly specific for select mRNAs, not only regulated in the producing cell, but by an intercellular signal. In this context, it is unlikely that

https://doi.org/10.1038/s41467-026-71740-1

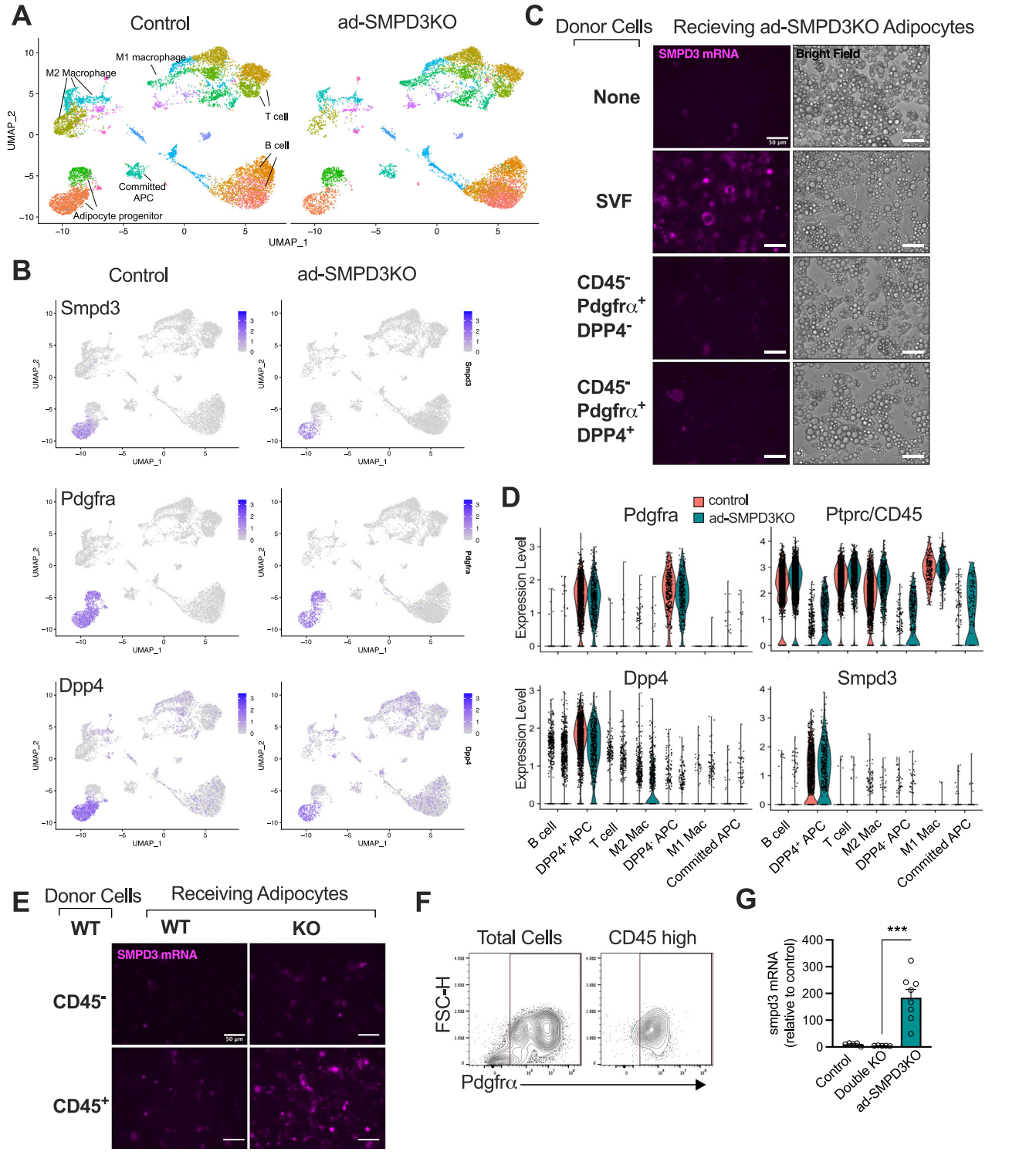

Fig. 4 | Identification of the Smpd3 mRNA donor cell. A UMAP plot of SVF cells from the sWAT of control and ad-SMPD3KO mice. **B** Distribution of Smpd3, Pdgfra, and Dpp4 mRNA expression. **C** SVF cells, PDGFRα^{+}/DPP4$^{+/-}$ cells were transfected with the Smpd3 MB, seeded into the upper chamber of a transwell plate, and co-cultured with mature adipocytes of the indicated genotypes. Adipocyte MB fluorescence was imaged at 40X. Representative of $n = 5$, 3 independent experiments. **D** scRNAseq gene expression in the indicated cell types. **E** CD45$^{+/-}$ cells co-cultured with adipocytes as in C. Representative of $n = 5$, 2 independent experiments. **F** Flow cytometric analysis of pdgfrα in sorted sWAT CD45^{+} cells following 2 days of culture. **G** Smpd3 mRNA in sWAT adipocytes purified from control, ad-SMPD3KO, and double KO (ad-SMPD3KO + Pdgfrα cre) mice ($n = 5$, $P = 0.0002$). Data are presented as mean ± s.e.m. Statistics by one-way ANOVA (Holm-Sidak test for multiple comparisons).

this mechanism of Smpd3 mRNA packaging into EVs by preadipocytes is driven by an intrinsic characteristic of the mRNA, like a 3' UTR consensus sequence. Instead, signaling-induced mRNA modifications, such as uridylation or methylation, or post-translational modifications of RNA-binding proteins would be expected to mediate packaging into EVs. Although EV RNAs are enriched or depleted of specific modifications compared to cellular RNAs, the direct role of these modifications in RNA sorting into EVs is not established[17]. The phenomenon

https://doi.org/10.1038/s41467-026-71740-1

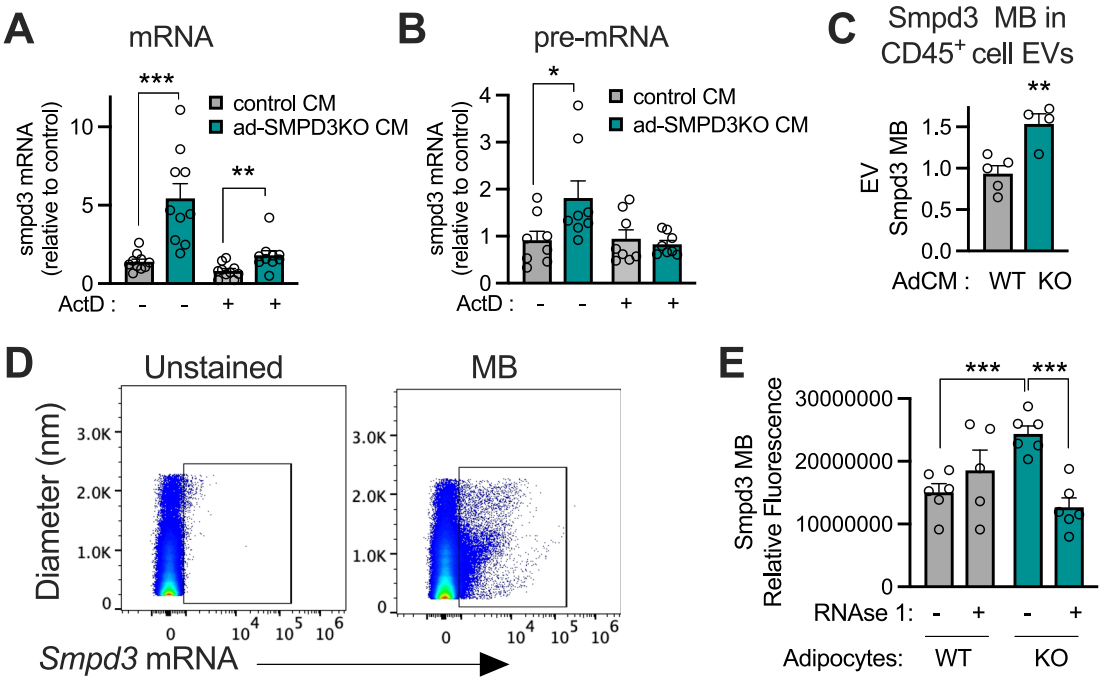

Fig. 5 | Smpd3 mRNA is transferred from CD45⁺ cells to adipocytes. A, B CD45⁺ cells treated with conditioned media (CM) from control or ad-SMPD3KO adipocytes for 24 h with or without 5 μM actinomycin D (ActD). Smpd3 mature mRNA (**A**) or pre-mRNA (**B**) was quantified by qPCR ($n = 8$). A. Control vs. KO CM - actD, $P = 0.0005$; Control vs. KO CM + actD, $P = 0.008$. B. Control vs. KO CM - actD, $P = 0.045$. **C** CD45⁺ cells transfected with the molecular beacon (MB) were treated with control or ad-SMPD3KO CM for 24 h. The media was replaced and 24 h later harvested to quantify EVs positive for the MB by flow cytometry (WT $n = 5$, KO $n = 4$, $P = 0.0058$). **D** A representative flow cytometry dot from (**C**). The side scatter detector was calibrated to estimate EV size. **E** CD45⁺ cells were transfected with the Smpd3 MB, seeded into the upper chamber of a transwell plate, and co-cultured with mature adipocytes of the indicated genotypes. Where indicated, RNAse1 was added to the shared media (100 μg/ml). Adipocyte MB fluorescence is displayed (WT+ $n = 5$; WT- $n = 6$ vs. KO- $n = 6$, $P = 0.0003$; KO- $n = 6$ vs. KO+ $n = 6$; $P < 0.0001$). Data are presented as mean ± s.e.m. Statistics by student's t-test (A-C) or one-way ANOVA (Holm-Sidak test for multiple comparisons; **E**).

described here is likely to have wider implications and apply more broadly to other targets. This could not only have consequences for preclinical gene manipulation in adipocytes but could also have clinical relevance in the context of disease-associated changes in the expression of a specific gene. As such, our observations break new ground in terms of adipocyte-specific gene manipulations. It sets adipose tissue apart from other tissues (such as the liver, where this phenomenon is not observed). However, we cannot rule out that this phenomenon occurs in other settings beyond adipose tissue. Our preliminary data suggest that, particularly, G-protein-coupled receptors (GPCRs) may be prone to this process. Our preliminary data suggest a very similar phenomenon for the adipocyte-specific gene disruptions of the Gastric Inhibitory Polypeptide Receptor (GIPR) and the Glucagon Receptor (GcgR) (Jiahui Luo, May-Yun Wang, and Philipp Scherer, manuscript in preparation). Our observations here establish a new phenomenon and shed new light on the complex cross-talk between the stromal vascular cells and adipocytes in adipose tissue.

Methods

Animals

All procedures performed on animals were approved by the Institutional Animal Care and Use Committee (IACUC) of the UT Southwestern Medical Center at Dallas and the Washington University in St. Louis School of Medicine. Mice were housed in a barrier facility with a 12-hour light/dark cycle and an average ambient temperature of 25 degrees celcius. All experiments were conducted using littermate-controlled male mice. Control and transgenic mice were co-housed. Mouse lines used in these studies included the 1) Smpd3^{flox} mice (this study), 2) adipocyte-specific adiponectin-Cre mice (B6;FVB-Tg(Adipoq-cre)1Evdr/J; The Jaxson Laboratory Stock No: 028020), 3) adipocyte-specific adiponectin-rtTA mice[18], 4) hepatocyte-specific albumin-Cre mice (The Jackson Laboratory, B6.Cg-Speer6-ps1Tg(Alb-cre)21Mgn/J, Stock No: 003574), 5) whole-body Rosa26-rtTA/R26-M2rtTA) (The Jackson Laboratory, B6.Cg-Gt(ROSA)26Sortm1(rtTA*M2) Jae/J, Strain: 006965), and 5) the TRE-Cre mice (TRE-Cre; B6.Cg-Tg(tetO-cre)1Jaw/J, No. 006234, JAX). Pdgrα-Cre was obtained from The Jackson Laboratory (Strain #:013148). Mice were euthanized with isoflurane followed by cervical dislocation. All mice used in this study were male.

Generation of the Smpd3 floxed line

Smpd3^{flox} mice were generated using CRISPR/Cas9-based genome editing. Two guide RNA sequences (GAGCAGGCTGCACGCGGATGAGG; GGAATCCTCACTCGCTTGATGGG) were designed in silico using CRISPOR to target sequences flanking exon 3. Single-stranded DNA repair templates containing 80 bp homology arms and a loxP sequence were synthesized as IDT ultramers. Guides, tracRNA, ssDNA repair template, and Cas9 protein (IDT) were mixed by the UT Southwestern Transgenic Core for pronuclear injection. We used the following primers to genotype the Smpd3^{flox} (230 bp) and non-modified (190 bp) alleles: 5'AGCTCCTGCCAACCCTTATT3'; 5'ACAGGTCGCTCCCACTCTAC3'.

Isolation of stromal vascular cells (SVF), mature adipocytes, and differentiation of adipocytes from SVF – Subcutaneous fat pads (sWAT) were dissected from 4–6 week-old mice. The tissues were minced and digested for 1 h at 37 °C in buffer containing 100 mM HEPES, 120 mM NaCl, 50 mM KCl, 1.5% BSA, 5 mM glucose, 1 mM calcium, and 1 mg/ml collagenase D (Sigma 11088882001). The dispersed tissue was then filtered through a 100 μm cell strainer and centrifuged at 600 × *g* for 5 min at 4 °C. Mature, floating adipocytes and pelleted

SVF were washed with 1 ml PBS and stored for RNA isolation. For culture, the SVF cells were resuspended in culture media (DMEM/F12 media containing 10% FBS, GlutaMax, 1X penicillin-streptomycin and gentamicin) and filtered through a 45 μm cell strainer. Cells were centrifuged again as described above. The pelleted cells were resuspended in culture media and grown at 37 °C, 5% CO_2. For in vitro differentiation experiments, SVF cells were allowed to grow to ~95% confluency. Adipogenesis was induced by culture media supplemented with 500 μM 3-isobutyl-1-methylxanthine (IBMX; Sigma I7018), 1 μM dexamethasone (Sigma D1756), 5 μg/ml Insulin (Sigma I6634) and 1 μm rosiglitazone (Sigma R2408) for 2 days. Following the 2 days of induction, cells were maintained in media containing only 5 μg/ml Insulin. Doxycycline (Sigma D9891) treatments were performed for 1–4 days at 1 μg/mL before media and cell harvest or co-culture for molecular beacon experiments at day 8 of differentiation. Where indicated, cells were lifted off the plate with trypsin. Mature adipocytes and non-differentiated stromal cells were separated by centrifugation at 600 x *g* for 5 min. Both the stromal cell pellet and floating adipocytes were washed with PBS and stored for RNA isolation.

Western Blot

Mature floating adipocytes were isolated from the inguinal fat pad of mice as described in above. Adipocytes were homogenized in ice-cold buffer (10 mM MOPS, 1 mM EDTA, 210 mM mannitol, and 70 mM sucrose, pH 7.4) using a Potter-Elvehjem homogenizer. The homogenate was centrifuged for 5 min at 600 xg, 4 °C. The resulting supernatant was centrifuged for 15 min at 10,000 xg. The supernatant was centrifuged at 60, 000xg for 30 min to pellet membranes. Protein was extracted from the membrane isolate, and RIPA buffer was added to the homogenate (10mM Tris-HCl, 2mM EDTA, 0.3% NP40, 0.3% deoxycholate, 0.1% SDS, and 140mM NaCl, pH 7.4). 20–50 μg/lane of supernatant protein was separated by SDS-PAGE (Thermo Fisher, NP0335BOX) and transferred to a nitrocellulose membrane. The blots were then incubated overnight at 4 °C with an anti-Smpd3 antibody (Santa Cruz Biotechnology, sc-166637) in a 1% BSA PBST blocking solution. The Odyssey Infrared Imager was used to visualize Western blots with Li-Cor IRDye secondary antibodies.

siRNA knockdown of SMPD3

Adipogenesis was induced in SVF as described in the "Isolation of stromal vascular cells (SVF), mature adipocytes, and differentiation of adipocytes from SVF" section. At day 3 of differentiation, adipocytes were reverse-transfected with smpd3 siRNAs. A 24-well culture plate was coated with 0.2% gelatin for 30 min at 37 degrees. Gelatin was removed, and the plate was dried. The transfection mix was made by combining lipofectamine RNAiMax (ThermoFisher, 13778100) with 2 siRNAs, 100 nM each (ThermoFisher s81737 and s81738) or 200 nM scramble siRNA (ThermoFisher 4390843) according to the manufacturer's instructions. 75 μl of transfection mix was added to each well and incubated at room temperature for 20 min. Adipocytes were detected from the plate with trypsin, pelleted at 500xg for 5 min at room temperature and re-suspended in culture media containing insulin (5 μg/ml) and no antibiotics. Adipocytes were seeded at 1 ×10^6 cells per gelatin-coated well containing the transfection mix. Adipocytes maintained ~80% differentiation rate after seeding. 3 days later adipocytes were used for experiments.

Fluorescence activated cell sorting (FACS) and bead sorting of SVF

SVF cells were collected as described above. For FACs-based sorting, SVF cells were resuspended in 200 μl PBS supplemented with 2% FBS and 2 mM EDTA (FACS buffer). CD16/CD32 Fc Block was added to the cells (1:200, BD Biosciences 553142 clone 2.4G2) for 10 min at 4 °C. An antibody cocktail was added to the cells and incubated for 15 min at 4 °C. The antibody cocktail consisted of anti-CD45 FITC (1:200; BD Biosciences 553080), anti-CD31 FITC (1:200 BioLegend 558738), anti-CD140a (PDGFα) PE (1:50; BioLegend 135905), and anti-CD26 (DPP4) BV421 (1:100; BD Biosciences 740021). Cells were washed with FACS buffer and sorted with a Cytek Aurora CS. The sorted populations were $CD45^-$, $CD31^-$, $PDGFR\alpha^+$, and either $DPP4^-$ or $^+$ (Supplementary Fig. 3). Cells were seeded in DMEM/F12 media containing 10% FBS, GlutaMax, 1X penicillin-streptomycin and gentamicin $CD45^+$ cells were bead-sorted using the MACS system (Miltenyl Biotec; CD45 microbeads 130-052-301 and MS column 130-042-201) per the manufacturer's instructions. Bead-sorted $CD45^+$ cells were cultured in DMEM/F12 media containing 10% FBS, GlutaMax, 1X penicillin-streptomycin, and gentamicin. This culture medium was chosen to match our SVF culture, where we know the cell population(s) responsible for Smpd3 mRNA transfer can propagate.

Adipose tissue small EVs (ATsEV) isolation

ATsEVs from the sWAT pad were isolated as previously published[10]. This method yields EVs that are enriched for EV markers and depleted of cellular proteins[10]. Furthermore, these EVs are between 50–300 nm in size by nanoparticle tracking analysis (ZetaView, Particle Metrix) and have the expected morphology by electron microscopy. Briefly, mice to be used for sEV isolation were perfused through the left ventricle of the heart with 3 ml ice cold PBS, to removed blood from the tissue. The inguinal fat pads from 3–5 mice were combined and digested as described above for the isolation of primary cells from adipose tissue. Special care was taken not to mince the tissue too finely as to avoid excessive cell rupture. Samples were diluted 1:1 in PBS containing 2 mM EGTA to inhibit collagenase activity. Following centrifugation at 600 g for 5 min at room temperature, the floating adipocytes were removed and discarded. The supernatant containing the sEVs was transferred into a 50 ml centrifuge tube and centrifuged at 1200 × *g* at 4 °C for 15 min. The supernatant was centrifuged again at 10,000 × *g* at 4 °C for 15 min. The resulting supernatant was then filtered through a 0.22 μm syringe-driven filter to remove any contaminating microvesicles and any remaining cellular debris. Clarified samples were then concentrated to 250 μl using a 100 KD MWCO Amicon Ultra-15 centrifugal filter units and diluted to 10 ml in PBS. Samples were then centrifuged in a fixed angle rotor at 100,000× *g* for 1.5 h to pellet sEVs. The pellet was washed in 10 ml PBS and centrifuged again at 100,000× *g* for 1.5 h. The pellet was resuspended in the lysis buffer from the RNAqueous Micro Total RNA Isolation Kit (ThermoFisher AM1931) for qPCR analysis or 4% paraformaldehyde for electron microscopy.

Electron microscopy of ATsEVs

A total of 2 μl of the sEV preparation was fixed in 20 μl freshly prepared and 0.2 μm filtered 4% paraformaldehyde. 10μl of the fixed sEV solution was transferred to each Formvar-carbon-coated (200μ Cu) electron microscopy grid. The grids were covered and incubated for 10 minutes. The grids were washed once with distilled water and stained with 2% uranyl acetate before imaging. Imaging was performed on a JEOL 1400plus electron microscope.

qPCR

RNA from cells or tissue was isolated with the Qiagen RNeasy kit per the manufacturer's protocol. In the column, DNAse digestion was performed. For ATEVs RNA was isolated according to the manufacturer's instructions for the RNAqueous Micro Total RNA Isolation Kit (ThermoFisher AM1931), including the genomic DNA digestion step. RNA yield and quality were determined using a NanoDrop or the BioTek Take3 plate. cDNA was prepared by reverse transcribing 1 μg of RNA from cells or ~25 ng RNA for EVs with the iScript cDNA Synthesis Kit (BioRad 1708890). A SYBR green method for qPCR was used (ThermoFisher A25742). Primers are listed in Table S1. All primers were purchased from Sigma Aldrich. Gene expression was calculated by the

standard threshold cycle method using B2m as a housekeeping gene for cells and tissues, and Gapdh for EVs.

Nuclei enrichment and One-Step qPCR

Mature floating adipocytes were isolated from the inguinal fat pad of mice as described in above. Adipocytes were homogenized in ice-cold homogenization buffer (20mM HEPES, pH 7.4, 250mM sucrose, 10mM KCl, 2mM MgCl2, 1mM EDTA, and 1mM EGTA) with a Potter-Elvehjem homogenizer. Nuclei were pelleted by centrifugation at 750 g for 5 min. The pellet was resuspended in ice-cold homogenization buffer and pelleted again at 750 g for 5 min. The final nuclei-enriched pellet was resuspended in qPCR lysis buffer (10 mM Tris pH 7.4, 150 mM NaCl, 0.25% NP-40) and the BioRad iTaq Universal SYBR green One-Step kit (cat #: 1725150) was used for qPCR. Genomic DNA was not eliminated in this protocol, however, the primers were designed to span the large intron between exon 2 and 3, to prevent detection of genomic DNA.

Single cell RNAseq

12-week-old male mice were fed a chow diet supplemented with 600mg/kg doxycycline for 2 weeks, and SVF cells were isolated from sWAT as described above. SVF was harvested from sWAT as described above. After centrifugation, the cells were resuspended in 2% FBS in PBS containing propidium iodide (PI; 1:400) and incubated for 15 min on ice. After washing, the cells were resuspended in 2% FBS in PBS for sorting of viable cells, PI^- cells. FACS was conducted with a BD Bioscience FACSAria cytometer at the Flow Cytometry Core Facility at UT Southwestern. Sorted live cells were immediately processed for single-cell RNA library preparation using the 10x Genomics Single Cell 3′ (v3.1) kit according to the manufacturer's instructions. 10,000 cells were partitioned into droplets containing a barcoded bead, a single cell, and reverse transcription enzyme mix using the Chromium Controller instrument (10x Genomics). This was followed by cDNA amplification, fragmentation, end repair, and A-tailing, adaptor ligation, and index PCR. Cleanup and size selection were performed using Dynabeads MyOne Silane beads (Thermo Fisher Scientific) and SPRIselect Reagent beads (Beckman Colter). Libraries were sequenced on an Illumina NextSeq 500 High Output (400 M) by the UT Southwestern McDermott Center Next Generation Sequencing Core.

Data analysis analyses of single-cell transcriptomes

Cell Ranger 5.0.1 (10x Genomics, https://www.10xgenomics.com/) was used to process the raw sequencing data. BCL files were converted to FASTQ files and aligned to the mouse (mm10) reference transcriptome. A unique molecular identifier and a valid cell barcode were used to quantify transcript counts of each cell. The gene expression matrix from Cell Ranger was used as input to the Seurat R package (v4.0.2) for downstream analysis. Cells with fewer than 250 genes per cell and high mitochondrial gene content were filtered out. The global-scaling normalization method LogNormalize was used for normalization. A subset of genes exhibiting high variation across the single cells was determined. The highly variable genes were calculated using the FindVariableFeatures module. The Shared Nearest Neighbor (SNN) graph was constructed with the FindNeighbors module by determining the k-nearest neighbors of each cell. The clusters were then identified by optimization of SNN modularity using the FindClusters module. We obtained 22 clusters with a resolution of 0.8. Clusters were annotated manually and with ScType[19] on the basis of known gene markers specific to various cell types. Differential expression analysis, clusters visualization, and plotting were all performed with Seurat.

ATsEV RNA Sequencing

RNA was isolated from ATsEVs using the RNAqueous Micro Total RNA Isolation Kit (ThermoFisher AM1931), and genomic DNA was eliminated by digestion. ~2 ng of RNA from each sample was submitted to the Genome Access Technology Center at the McDonnell Genome Institute at Washington University in St. Louis. Total RNA Integrity was determined using the Agilent Bioanalyzer. ds-cDNA was prepared with the SMARer Ultra Low RNA kit for Illumina Sequencing (Takara-Clontech). The Covaris E220 sonicator was used to fragment the cDNA (peak incident power 18, duty factor 20%, cycles per burst 50 for 120 s). cDNA was then blunt ended. An A base was added to the 3′ ends, and Illumina sequencing adapters were ligated to the ends. After amplification, fragments were sequenced on an Illumina NovaSeq X Plus using paired-end reads extended 150 bases.

Read count quantification over Smpd3 introns and exons

Total RNA was extracted from adipocytes from control and ad-SMPD3KO mice using RNAqueous Micro Total RNA Isolation Kit (ThermoFisher AM1931), followed by ribosomal RNA (rRNA) depletion with the NEBNext® rRNA Depletion Kit v2 (Human/Mouse/Rat; NEB, E7400). rRNA-depleted RNA was used for library preparation with the NEBNext® Ultra™ RNA Library Prep Kit for Illumina® (NEB, E7530) following the manufacturer's protocols. Libraries were indexed, pooled, and sequenced on an Illumina NovaSeq 6000 platform. Base calling and demultiplexing were performed using Illumina's bcl2fastq software and a custom Python demultiplexing script, allowing a maximum of one mismatch in the index read. Adapter trimming was conducted using TrimGalore (v0.6.0), and reads were aligned to the GENCODE Mouse Release M37 (GRCm39) reference genome using STAR (v2.5.1a). Only uniquely mapped reads were retained for subsequent analysis. Smpd3 intron and exon coordinates were obtained from the UCSC Table Browser. Quantification was performed using a custom script: read pairs were classified as intronic if both reads mapped within the same Smpd3 intron, and exonic if either read overlapped with any Smpd3 exon.

Adipose tissue transplantation

Whole-body SMPD3KO mice (rosa26 rtTA x TRE-Cre x $Smpd3^{flox/flox}$) were placed on a diet containing 600 mg/kg doxycycline for 2 weeks to induce the global knockout. At 6 weeks old, a donor (knockout) and a recipient (WT control) mouse were anesthetized with isoflurane. The inguinal fat pad was resected from the donor mouse and washed with sterile saline. The tissue was cut into ~ 3 mm cubes. A small incision was made in the skin above the inguinal fat pad of the recipient mouse. Following light wounding of the recipient fat pad, the donor tissue pieces were secured to it with Vicryl (polyglactin 910) sutures (5-0, J303H) and the skin was sutured closed. Tissue pieces were spread out to avoid aggregation and necrosis. Donor mice were then perfused with 10% formalin, the remaining inguinal fat pad was removed, and processed for RNAscope. Donor mice were then euthanized by isoflurane and cervical dislocation, and recipient mice allowed to recover with on a diet containing 600 mg/kg doxycycline for 2 weeks. After recovery, mice were euthanized as above and perfused with 10% formalin in PBS. The inguinal fat pad was collected, and the donor tissue was carefully removed and processed for RNAscope.

RNAscope

RNAscope multiplex fluorescent assay was performed by the UT Southwestern Metabolic Phenotyping Core to simultaneously detect Smpd3 and Adipoq transcripts in paraffin-embedded adipose tissue sections. Slides were deparaffinized and treated according to the manufacturer's instructions (Advanced Cell Diagnostics, Inc. (ACD), California) using the RNAscope® Multiplex Detection Kit V2 (cat# 323110). Probes (Mm-Adipoq-O2-C1 cat# 1244281; Mm-Smpd3-C3 cat# 815591-C3] were applied at 40 °C for 2 h. Signal was detected using Opal dyes 520 and 570 (Akoya Biosciences). Slides were counterstained with DAPI before mounting with ProLong™ Gold Antifade (Cat# P36930) and a coverslip over the tissue section. Confocal images were taken by a blinded operator.

Molecular beacon transwell assay

The molecular beacon (MB) was designed to have complementary sequence with Smpd3 mRNA. The sequence was blasted to verify Smpd3 mRNA specificity. The MB was synthesized by Integrated DNA Technologies (IDT) with AlexaFluor^{647} on the 5′ end and the Black Hole Quencher-2 (BHQ-2) on the 3′ end (5′Alexa Fluor647-mCmGmCmGmAmUmC*mU*mA*mC*mU*mC*mC*mU*mA*mC* mU*mC*mC*mC*mG*mG*mC*mU*mA*mG*mA*mA*mG*mA*mC*mA* mG*mAmUmCmGmCmGm-3BHQ-2 3′; where "m" indicates O-methylated bases and * denotes phosphorothioate linkage modification. Cells were transfected with MB using microporation (Thermo Fisher Scientific Neon Transfection System). All donor cells were used for co-culture with adipocytes at passage 1. 50,000 cells were re-suspended in R buffer with 1–5 μM MB, depending on the lot. The Neon was set at 1300 V, 30 ms, 1 pulse for transfection of all cells except CD45$^+$ cells which were microporated at 1900 V, 20 ms, 1 pulse. Following microporation, the 50,000 cells were seeded into the upper chamber of a transwell with a pore size of 0.4 μM. Following overnight recovery in DMEM/F12 media containing 10% FBS, GlutaMax, 1X penicillin-streptomycin, and gentamicin, the insert was washed 3 times with PBS and placed into a 24-well plate containing differentiated adipocytes. Adipocytes were at day 6 of differentiation at the time of co-culture. The adipocytes were treated with 1 μg/ml doxycycline in 500 μl treatment media, FluoroBrite DMEM containing 1X penicillin-streptomycin and 1% EV-depleted FBS (System Biosciences; EXO-FBSHI-250A-1) for 24 h before co-culture. The adipocyte media was not changed before the inserts were placed in the wells. 100 μl of treatment media was added to the insert. Cells were co-cultured for 24 h before visualization of adipocytes by fluorescent microscopy. For validation experiments, SVF was seeded in a black 96-well plate for better imaging. Where indicated, RNAse 1 was added to the bottom chamber to a final concentration of 100 μg/ml. Images were taken and analyzed blindly by ImageJ.

Nano flow cytometry of EVs

Immune cell EVs were analyzed using a Cytek Northern Lights flow cytometer with enhanced small-particle detection. Samples were serially diluted to ensure single particle detection and prevent swarming. Optimal concentrations were indicated by an abort rate that was less than 10% of the event rate. The trigger channel was set to the violet (405) side scatter (SSC), and the threshold was set at 600 arbitrary units. The SSC detector was calibrated using Rosetta Calibration (Exometry). The software approximates particle size using Mie theory with beads of known refractive index.

Statistics

All data is presented as mean ± SEM. $^*p < 0.05$, $^{**}p < 0.01$ and $^{***}p < 0.001$ by two-tailed Student's t test. A p-value < 0.05 was determined to be statistically significant. For all mouse studies, the n value corresponds to individual mice of a given treatment. For cell studies, the n value corresponds to cells from individual mice. Each data point in the graphs is a separate n. Data was analyzed using Prism GraphPad Software, ImageJ, and FlowJo.

Reporting summary

Further information on research design is available in the Nature Portfolio Reporting Summary linked to this article.

Data availability

All data supporting the results of this study can be found in the article, supplementary information, and Source Data File. The sequencing data has been deposited in the GEO database under accession numbers GSE319159 (scRNAseq) and GSE319160 (RNAseq). Source data are provided with this paper.

References

1. van Niel, G., D'Angelo, G. & Raposo, G. Shedding light on the cell biology of extracellular vesicles. *Nat. Rev. Mol. Cell Biol.* **19**, 213–228 (2018).
2. Fu, S. et al. Extracellular vesicles in cardiovascular diseases. *Cell Death Discov.* **6**, 68 (2020).
3. Raghav, A. et al. Extracellular vesicles in neurodegenerative diseases: A systematic review. *Front Mol. Neurosci.* **15**, 1061076 (2022).
4. Isaac, R., Reis, F. C. G., Ying, W. & Olefsky, J. M. Exosomes as mediators of intercellular crosstalk in metabolism. *Cell Metab.* **33**, 1744–1762 (2021).
5. Xu, R. et al. Extracellular vesicles in cancer - implications for future improvements in cancer care. *Nat. Rev. Clin. Oncol.* **15**, 617–638 (2018).
6. Crewe, C. & Scherer, P. E. Intercellular and interorgan crosstalk through adipocyte extracellular vesicles. *Rev. Endocr. Metab. Disord.* **23**, 61–69 (2022).
7. Crewe, C. et al. Deficient caveolin-1 synthesis in adipocytes stimulates systemic insulin-independent glucose uptake via extracellular vesicles. *Diabetes* **71**, 2496–2512 (2022).
8. Crewe, C. et al. Extracellular vesicle-based interorgan transport of mitochondria from energetically stressed adipocytes. *Cell Metab.* **33**, 1853–1868 e1811 (2021).
9. Trajkovic, K. et al. Ceramide triggers budding of exosome vesicles into multivesicular endosomes. *Science* **319**, 1244–1247 (2008).
10. Crewe, C. et al. An endothelial-to-adipocyte extracellular vesicle axis governed by metabolic State. *Cell* **175**, 695–708 e613 (2018).
11. O'Brien, K., Breyne, K., Ughetto, S., Laurent, L. C. & Breakefield, X. O. RNA delivery by extracellular vesicles in mammalian cells and its applications. *Nat. Rev. Mol. Cell Biol.* **21**, 585–606 (2020).
12. Bonsergent, E. et al. Quantitative characterization of extracellular vesicle uptake and content delivery within mammalian cells. *Nat. Commun.* **12**, 1864 (2021).
13. Merrick, D. et al. Identification of a mesenchymal progenitor cell hierarchy in adipose tissue. Science **364**, https://doi.org/10.1126/science.aav2501 (2019).
14. Prieto-Vila, M., Yoshioka, Y. & Ochiya, T. Biological functions driven by mrnas carried by extracellular vesicles in cancer. *Front Cell Dev. Biol.* **9**, 620498 (2021).
15. Tomita, T. et al. Extracellular mRNA transported to the nucleus exerts translation-independent function. *Nat. Commun.* **12**, 3655 (2021).
16. Ratajczak, J. et al. Embryonic stem cell-derived microvesicles reprogram hematopoietic progenitors: evidence for horizontal transfer of mRNA and protein delivery. *Leukemia* **20**, 847–856 (2006).
17. Dellar, E. R., Hill, C., Melling, G. E. & Carter, D. R. & Baena-Lopez, L. A. Unpacking extracellular vesicles: RNA cargo loading and function. *J. Extracell. Biol.* **1**, e40 (2022).
18. Wang, Z. V., Deng, Y., Wang, Q. A., Sun, K. & Scherer, P. E. Identification and characterization of a promoter cassette conferring adipocyte-specific gene expression. *Endocrinology* **151**, 2933–2939 (2010).
19. Ianevski, A., Giri, A. K. & Aittokallio, T. Fully-automated and ultra-fast cell-type identification using specific marker combinations from single-cell transcriptomic data. *Nat. Commun.* **13**, 1246 (2022).

Acknowledgements

Funding: National Institutes of Health grants R00-DK122019, 1R01DK137791, 1R21EB035738, DRC at Washington University (NIH P30DK020579), American Heart Association (AHA 23IPA1054013) (CC). R01-DK55758, R01-DK099110, R01-DK127274, R01-DK143576, R01-DK131537, P01-AG051459, the UTSW NORC P30-DK127984 (P.E.S.). R01-DK114036, R01-DK130892, R01-DK136592 (CL). The authors thank the UT

Southwestern Metabolic Phenotyping Core (RRID: SCR_026404) for its assistance with metabolic phenotyping.

Author contributions

Conceptualization: C.C. and P.E.S. Investigation: C.C., C.M.G., T.O., S.C., J.B.F., M.Y.W., S.T., Y.L.P., M.R., S.A.P., Z.Y., Y.C.Z., A.L., L.G., C.K.C., and C.L. Data curation: C.C., Z.Y., C.X., and C.K.C. Formal analysis: C.C., Z.Y., C.X., A.L. Visualization: C.C., Z.Y., C.X., T.O., and P.E.S. Funding acquisition: C.C. and P.E.S. Supervision: C.C. and P.E.S. Writing-original draft: CC. Writing - review and editing C.C. and P.E.S.

Competing interests

The authors declare no competing interests.

Additional information

Supplementary information The online version contains supplementary material available at https://doi.org/10.1038/s41467-026-71740-1.

Correspondence and requests for materials should be addressed to Clair Crewe.

Peer review information *Nature Communications* thanks Baisong Lu who co-reviewed with Balqees Khaderand the other anonymous reviewer(s) for their contribution to the peer review of this work. A peer review file is available.